

Thermodynamic Calculations for Molecules with Asymmetric Internal Rotors—Application to 1,3-Butadiene

BRYAN M. WONG,¹ SUMATHY RAMAN²

¹Department of Chemistry, Massachusetts Institute of Technology, Cambridge, Massachusetts 02139

²Department of Chemistry, Oakwood College, Huntsville, Alabama 35896

Received 4 July 2006; Revised 4 August 2006; Accepted 28 August 2006

DOI 10.1002/jcc.20536

Published online 16 January 2007 in Wiley InterScience (www.interscience.wiley.com).

Abstract: We present quantum mechanical partition functions, free energies, entropies, and heat capacities of 1,3-butadiene derived from *ab initio* calculations. Our technique makes use of a reaction path-like Hamiltonian to couple all 23 vibrational modes to the large-amplitude torsion, which involves heavy asymmetric functional groups. *Ab initio* calculations were performed at the B3LYP, MP2, and CCSD(T) levels of theory and compared with experimental values as a reference case. By using the *ab initio* potentials and projected frequencies, simple perturbative expressions are presented for computing the couplings of all the vibrational modes to the large-amplitude torsion. The expressions are particularly suited for programming in the new STAR-P software platform which automatically parallelizes our codes with distributed memory via a familiar MATLAB interface. Using the efficient parallelization scheme of STAR-P, we obtain thermodynamic properties of 1,3-butadiene for temperatures ranging from 50 to 500 K. The free energies, entropies, and heat capacities obtained from our perturbative formulas are compared with conventional approximations and experimental values found in thermodynamic tables.

© 2007 Wiley Periodicals, Inc. J Comput Chem 28: 759–766, 2007

Key words: internal rotation; large-amplitude torsion; butadiene; thermodynamic properties; partition function

Introduction

The pursuit and implementation of new approaches for calculating thermochemical properties from first principles has always been a topic of ongoing research.^{1–4} As advances in quantum chemical calculations have made it feasible to calculate potential energy surfaces accurately, the use of computational chemistry has become the method of choice for estimating free energies, equilibrium constants, and reaction rates. For example, energies for large molecules obtained from post-Hartree-Fock methods such as Møller-Plesset perturbation theories and coupled-cluster calculations are now commonplace in modern quantum chemistry.⁴ In particular, the widespread use of analytical gradients and second derivatives of the potential energy has allowed theoretical results to replicate and sometimes rival experimental thermodynamic data. Nevertheless, the raw results of *ab initio* electronic structure calculations always correspond to properties at absolute zero temperature, and statistical thermodynamics is required to obtain properties as functions of temperature.

In certain extreme situations, the *ab initio* results alone do not correspond to absolute zero conditions, and the conventional statistical thermodynamic formulas must also be corrected. The

most familiar case of this error arises when large-amplitude, internal motions of the nuclei are present in a molecule. For example, the most common vibrations of nuclei occur when the motions are localized close to the potential energy minima. These high-frequency modes are well-approximated as small-amplitude harmonic oscillations and zeroth-order vibrational states. However, in the case of large-amplitude motions, such as internal rotation or inversion, the motion extends over more than one potential energy minimum, and the normal-mode approximation is invalid. Uncertainties in treating these internal torsions and other anharmonic effects can be a significant error in thermodynamic and rate constant calculations.

The present paper focuses on the calculation of thermochemical properties where an asymmetric internal rotation is coupled to the other vibrational modes and to the overall external rotation in molecules. The conventional statistical mechanical approach to computing partition functions and thermochemistry of internal rotations is through the use of Pitzer-Gwinn tables^{5–7} or approximate analytical formulas. However, Pitzer also real-

Correspondence to: B. M. Wong; e-mail: usagi@mit.edu

ized that these protocols are only highly accurate when the moments of inertia for overall rotation are weakly dependent on the coordinates of internal rotation. To correct this inadequacy, we use the *ab initio* internal coordinate path Hamiltonian formalism of Tew et al.⁸ to compute thermochemical properties since analytical potentials are not available for most systems of interest. This work demonstrates that thermochemical properties can be easily computed from an *ab initio* coordinate path including harmonic fluctuations projected from this path.

We present 1,3-butadiene, C₄H₆, as a prototypical molecule with various types of complex couplings. The large-amplitude internal rotation of 1,3-butadiene requires alignment of conjugated π -orbitals, and the energetics and vibrational frequencies are strongly sensitive to variations in the torsional angle. For example, a reliable description of this torsion and its couplings is required to rationalize the thermodynamics and kinetics of the Diels–Alder reaction, a mechanism which still attracts interest in reaction dynamics.⁹ Furthermore, since the torsion involves asymmetric internal rotors, the geometries and the effective moment of inertia will also be strongly coupled to this internal coordinate. When the barriers to internal rotation are small in comparison with $k_B T$, one would expect the torsion to become a large-amplitude hindered internal rotor. The combination of large amplitude and strong coupling would be expected to lead to a break down in both the separability assumption and conventional thermodynamic formulas. We provide simple corrective formulas that can be easily implemented using high-level matrix manipulation languages, in particular the new parallelized version of STAR-P MATLAB.^{10,11} This method of calculation is useful since the familiar STAR-P MATLAB interface contains efficient, parallel, built-in functions that can be easily modified to use on other molecular systems. The examples presented allow the assessment of the accuracy of other conventional assumptions used in computing partition functions and thermochemical properties.

Hamiltonian

The theory of the internal coordinate path Hamiltonian is expressed in terms of a single large-amplitude coordinate s , its conjugate momentum \hat{p}_s ($= -i\hbar\partial/\partial s$), and the coordinates Q_k ($k = 1, 2, \dots, 3N-7$) and momenta \hat{P}_k ($= -i\hbar\partial/\partial Q_k$) of the orthogonal small-amplitude vibrational modes. A detailed description of the internal coordinate path Hamiltonian and its derivation has been given by Tew et al.⁸ Their formulation is closely related to the reaction path Hamiltonian by Miller, Handy, and Adams¹² with the exception that the internal coordinate path need not be exactly parallel to the minimum energy path. In the present work we use the internal coordinate path method, but the dense vibrational spectra of large molecules requires an approximate treatment for the other small-amplitude modes. As reported previously,¹³ the following approximations allow for the computation to be manageable: (1) the inertia tensor depends weakly on the small-amplitude coordinates Q_k , and only the terms in the inertia tensor that depend on the large-amplitude coordinate s are retained; (2) the Coriolis terms are linear in the small-amplitude coordinates Q_k , and their contribution to

the kinetic energy is neglected; (3) numerically enforcing the Eckart conditions minimizes many of the couplings between the large-amplitude motion and the overall rotation of the molecule. It follows from these approximations that the kinetic energy operator for total angular momentum $J = 0$ can be written in the following form (cf. eq. (10) of ref. 13)

$$\hat{T} = \frac{1}{2}\hat{p}_s I_{0ss}^{-1} \hat{p}_s + \frac{1}{2}\mu^{1/4} \left(\hat{p}_s I_{0ss}^{-1} \mu^{-1/2} \left(\hat{p}_s \mu^{1/4} \right) \right) + \frac{1}{2} \sum_{k=1}^{3N-7} \hat{P}_k^2, \quad (1)$$

where the scalar terms I_{0ss}^{-1} and μ are given by

$$I_{0ss}^{-1}(s) = \left(\sum_{i=1}^N \mathbf{a}'_i(s) \cdot \mathbf{a}'_i(s) \right)^{-1} \quad (2)$$

$$\mu(s) = I_{0ss}^{-1} \cdot \det(\mathbf{I}_0^{-1}), \quad (3)$$

and \mathbf{I}_0 is the normal 3×3 Cartesian inertia tensor along the path. The vectors \mathbf{a}_i ($= m_i^{1/2} \mathbf{r}_i$) are the mass-weighted Cartesian coordinates of the i th atom at a point on the path s with respect to the Eckart axis system, and $\mathbf{a}'_i = d\mathbf{a}_i/ds$. The corresponding potential energy can be expanded in terms of Q_k . In this work, only the term quadratic in the small-amplitude coordinates is retained since the anharmonic terms are rarely available for large polyatomics; therefore,

$$\hat{V} = V_0(s) + \frac{1}{2} \sum_{k=1}^{3N-7} \omega_k^2(s) Q_k^2, \quad (4)$$

where $V_0(s)$ is the energy along the internal coordinate path, and $\omega_k(s)$ is the frequency of mode k obtained by diagonalization of a projected Hessian matrix in the $3N-7$ small-amplitude degrees of freedom.

The simplest approximation to $\hat{H} = \hat{T} + \hat{V}$ is obtained by neglecting the s -dependence of the $\omega_k^2(s) Q_k^2$ term in eq. (4). The $J = 0$ Hamiltonian in this zeroth-order approximation is

$$\begin{aligned} \hat{H}^{(0)} = & \frac{1}{2}\hat{p}_s I_{0ss}^{-1} \hat{p}_s + \frac{1}{2}\mu^{1/4} \left(\hat{p}_s I_{0ss}^{-1} \mu^{-1/2} \left(\hat{p}_s \mu^{1/4} \right) \right) \\ & + V_0(s) + \frac{\hbar}{2} \sum_{k=1}^{3N-7} [\omega_k(s) - \omega_k(s_0)] \\ & + \frac{1}{2} \sum_{k=1}^{3N-7} [\hat{P}_k^2(s_0) + \omega_k^2(s_0) Q_k^2], \quad (5) \end{aligned}$$

where s_0 is the value of the internal coordinate corresponding to the most stable conformer of the molecule; i.e., V_0 has a global minimum at $s = s_0$. We denote this separable Hamiltonian in eq. (5) as a zeroth-order Hamiltonian and solve the more exact Hamiltonian given by eqs. (1) and (4) using perturbation theory. The term $\hbar/2 [\omega_k(s) - \omega_k(s_0)]$ is part of the effective potential energy since it adds no extra computational complexity and sim-

plifies our perturbative expressions. A convenient choice of basis for eq. (5) is given by the direct product

$$\left| \Psi_{m,\mathbf{n}}^{(0)}(s, Q_1, Q_2, \dots, Q_{3N-7}) \right\rangle = \left| \psi_m(s) \right\rangle \prod_{k=1}^{3N-7} \left| \chi_{n_k}(Q_k) \right\rangle, \quad (6)$$

where $\mathbf{n} = \{n_1, n_2, \dots, n_{3N-7}\}$ is a set of $3N - 7$ harmonic quantum numbers, $\psi_m(s)$ is the m th eigenfunction of the large-amplitude motion, and $\chi_{n_k}(Q_k)$ is a harmonic oscillator eigenfunction at $s = s_0$ with a number n_k of quanta in oscillator k . The zeroth-order Hamiltonian in eq. (5) can be solved by direct diagonalization using several basis functions in the large-amplitude coordinate s ; its solution is straightforward

$$E_{m,n_k}^{(0)} = E_m + \sum_{k=1}^{3N-7} \left(n_k + \frac{1}{2} \right) \hbar \omega_k(s_0), \quad (7)$$

where E_m is an eigenvalue of the large-amplitude motion operator (first four terms in eq. (5)), which is determined by solving the following matrix equation

$$\left\langle \psi_l(s) \left| \frac{1}{2} \hat{p}_s I_{0ss}^{-1} \hat{p}_s + \frac{1}{2} \mu^{1/4} \left(\hat{p}_s I_{0ss}^{-1} \mu^{-1/2} \left(\hat{p}_s \mu^{1/4} \right) \right) + V_0(s) \right. \right. \\ \left. \left. + \frac{\hbar}{2} \sum_{k=1}^{3N-7} [\omega_k(s) - \omega_k(s_0)] \right| \psi_m(s) \right\rangle - \delta_{l,m} E_m = 0. \quad (8)$$

The corrections due to the large-amplitude motion coupling with the $3N-7$ vibrational modes can be solved approximately using perturbation theory. Taking the separable Hamiltonian in eq. (5) to be the zeroth-order Hamiltonian, the approximate correction to the energy in eq. (7) is the average value of $\hat{H} - \hat{H}^{(0)}$ over the unperturbed states. In the representation of the chosen basis in eq. (6), the approximate corrections are

$$E_{m,\mathbf{n}}^{(1)} = \hbar \sum_{k=1}^{3N-7} \left\langle \psi_m(s) \left| \omega_k(s) - \omega_k(s_0) \right| \psi_m(s) \right\rangle n_k. \quad (9)$$

It should be noted that if the term $\hbar/2 [\omega_k(s) - \omega_k(s_0)]$ was not present in $\hat{H}^{(0)}$, the expression in eq. (9) would be proportional to $(n_k + [1/2])$ instead of just n_k . The inclusion of the term $\hbar/2 [\omega_k(s) - \omega_k(s_0)]$ in $\hat{H}^{(0)}$ makes the zeroth-order energies in eq. (7) more accurate for both the $n_k = 0$ and higher n_k states. Therefore, the corrected energy with this perturbative treatment is given by

$$E_{m,\mathbf{n}}^{\text{Pert}} = E_{m,\mathbf{n}}^{(0)} + E_{m,\mathbf{n}}^{(1)} \\ = E_m + \hbar \sum_{k=1}^{3N-7} \left\{ \left[\omega_k(s_0) + \left\langle \psi_m(s) \left| \omega_k(s) - \omega_k(s_0) \right| \psi_m(s) \right\rangle \right] n_k \right. \\ \left. + \frac{1}{2} \omega_k(s_0) \right\}. \quad (10)$$

In the results section, we utilize this perturbative expression to obtain thermochemical properties of 1,3-butadiene.

Ab Initio Calculations

All *ab initio* electronic structure calculations on 1,3-butadiene, C_4H_6 , were carried out with the Gaussian 03 package.¹⁴ A complete geometry optimization places the minimum energy of 1,3-butadiene to be in a *trans* isomeric form with a C_{2h} point group symmetry. In addition, 1,3-butadiene also exists as two equivalent stable *gauche* forms. Extensive theoretical^{15–18} and a few experimental^{19–20} studies have been carried out on this π -conjugated torsional potential energy surface. One of the most recent theoretical studies on 1,3-butadiene in the current literature is the investigation by Karpfen and Parasuk.¹⁸ Their analysis includes several *ab initio* calculations of the torsional potential performed at the MP2 and CCSD(T) levels of theory. In all cases they considered, the torsional energy profile follows the most stable *trans* conformation over a transition state and *gauche* minimum to the *cis* transition state. The most consistent and accurate *ab initio* energies are from their CCSD(T)/cc-pV5Z calculations which yield a 1014 cm^{-1} energy difference between the *trans* and *gauche* minima. The currently accepted experimental value is 989 cm^{-1} obtained from UV spectra.¹⁹

Since the focus of this work is to improve conventional assumptions for calculating partition functions and thermochemical properties, we do not intend to reproduce Karpfen and Parasuk's *ab initio* values exactly. Instead we wish to obtain reasonable results from a fairly accurate computational method which provides second derivatives. To this end, the relaxed geometry parameters and Hessian matrices were analyzed using second order Møller-Plesset perturbation theory (MP2) and density functional theory with the B3LYP hybrid density functional. The basis set used for both levels of theory was Dunning's correlation consistent triple-zeta basis, cc-pVTZ.²¹ The geometry optimizations for both the MP2 and B3LYP methods were carried out with the "OPT = verytight" option which converges root mean square forces to 0.00001 atomic units and root mean square displacements to 0.00004 atomic units. The force constant matrix was output by setting internal options using the "IOP(7/33 = 1)" keyword. In addition to these keywords, the "Int = Ultrafine" option must also be specified for density functional calculations. This additional selection is recommended when using the "OPT = verytight" option to minimize the low-frequency translational and rotational modes. CCSD(T) single-point energies were subsequently performed with the cc-pVTZ basis set at the MP2 and B3LYP optimized geometries.

For all levels of theory, the torsional potential was calculated by constraining the C=C–C=C dihedral angle at 10° increments and optimizing all other internal coordinates to minimize the total energy. At all intermediate geometries between the C_{2h} *trans* minimum and the C_{2v} *cis* maximum, molecular symmetry was constrained to a C_2 point group. The torsional potentials relative to the *trans* global minimum as obtained for B3LYP, MP2, CCSD(T)/B3LYP, CCSD(T)/MP2, and the experimental potential¹⁹ are shown in Figure 1. The differences between the CCSD(T)/B3LYP and CCSD(T)/MP2 potentials are unnoticeable at the scale of Figure 1 since the single-point energies do not differ by more than 20 cm^{-1} over the entire range. The large deviation of the B3LYP potential from the CCSD(T) energies is expected since it is well-known that DFT methods generally pre-

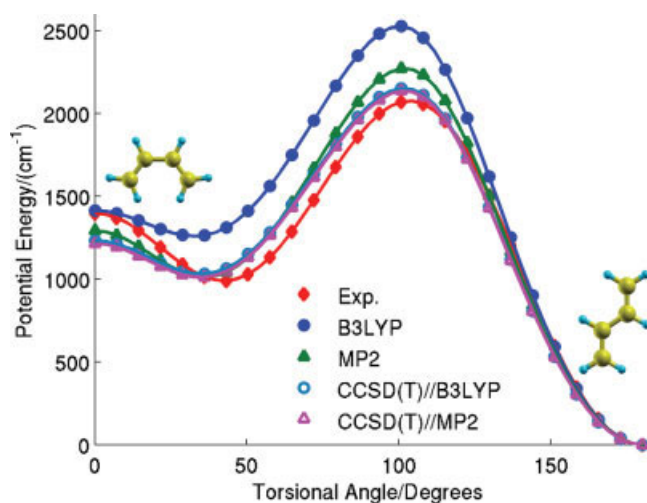


Figure 1. Experimental torsional potential of 1,3-butadiene compared with *ab initio* calculations from B3LYP, MP2, and CCSD(T) levels of theory.

dict higher *trans-gauche* barriers.²² At the MP2 level of theory, the barrier height is lower than the corresponding B3LYP energy, but there is still a significant reduction of the barrier height when the CCSD(T) method is employed. Of all the methods used in this work, we observe the best agreement between the CCSD(T)//MP2 potential and the experimental energy differences. The relative energy of the *gauche* form calculated with respect to the *trans* isomer was 1124 cm^{-1} at this level of theory with the cc-pVTZ basis. Although the *trans-gauche* barrier for CCSD(T)//MP2 is still 212 cm^{-1} higher than the experimentally derived value, this discrepancy is well-known and has been documented by others.¹⁸ In the remainder of this work, we will only utilize the geometries, energies, gradients, and force constant matrices obtained from the CCSD(T)//MP2 method in calculating torsional energies and thermochemical properties.

The torsional potential energy surface of 1,3-butadiene is invariant under the σ_h symmetry operation, and the C=C—C=C dihedral angle preserves this permutation symmetry of the true Hamiltonian. Therefore, the fully symmetric internal coordinate path, energies, gradients, and force constant matrices can be constructed with only the information from *trans* to *cis* by using permutation operations in a local frame. Each resulting geometry was translated to the center of mass frame, and all Cartesian components as a function of s were fit to a Fourier series. In this way, finite differences can be used to numerically solve for the Euler angles which rotate the Cartesian axes and force constant matrix to align the molecule along an Eckart frame.

We should also remember the ordering of the projected frequencies by diagonalization of the projected force constant matrix is arbitrary for each value of the dihedral angle. Introducing factors of -1 and re-labeling eigenvectors to maximize consecutive dot products generates a set of physically meaningful diabatic frequencies and orthogonal vibrational modes.²³ It is essential to obtain the correct ordering of frequencies and eigenvectors since it provides a correct model for the strong coupling between the torsional motion and other vibrational modes. This

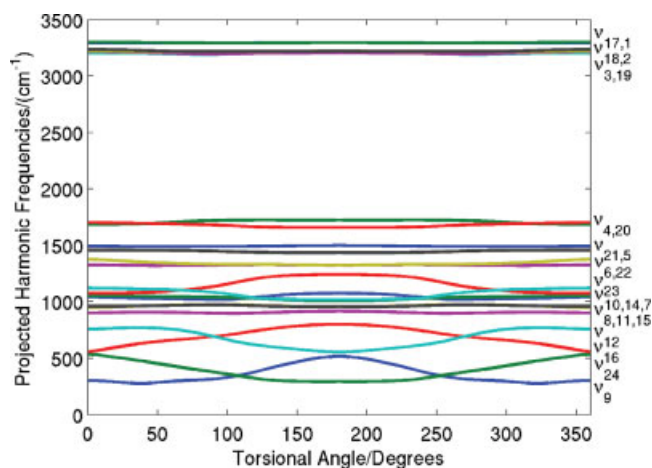


Figure 2. Projected harmonic frequencies for 1,3-butadiene computed as a function of the torsional angle. The lowest four frequencies, ν_{24} , ν_9 , ν_{12} , and ν_{16} , are highly coupled to the large-amplitude torsion.

is verified with our level of theory, and Figure 2 shows the strong variation of the projected harmonic frequencies as a function of the internal coordinate path. In other words, the harmonic wave numbers are not constant with respect to s , indicating a mixing of pure torsion with other vibrational modes.

Thermodynamic Calculations and Results

The $J = 0$ canonical partition function can be calculated by numerical summation over several torsional-vibrational energy levels and their perturbations (eq. (10)). The rovibrational energies

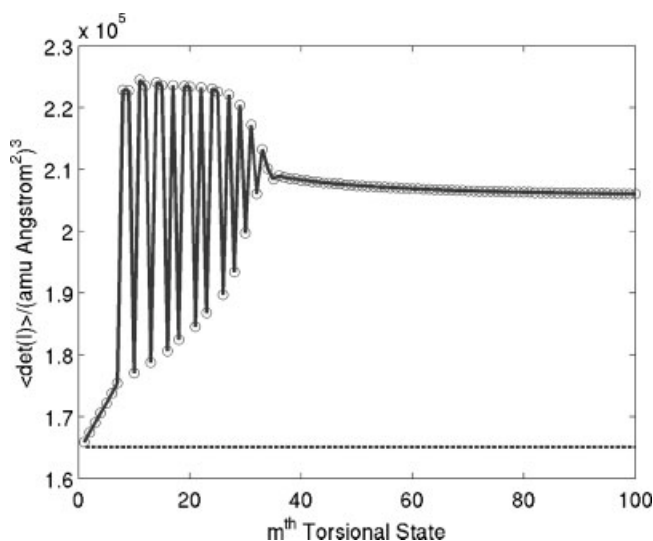


Figure 3. The lowest 100 effective products of inertia obtained by averaging $\det[\mathbf{I}_b(s)]$ across the torsional wavefunctions (cf. eq. (16)). The broken line indicates the numerical value of the equilibrium products of inertia $I_{0a}I_{0b}I_{0c}$ calculated at the *trans* global minimum of 1,3-butadiene.

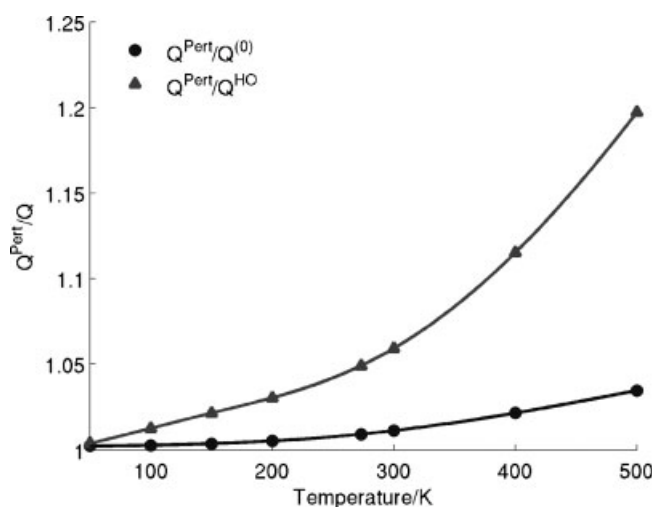


Figure 4. Ratios of partition functions $Q^{\text{Pert}}(T)/Q^{\text{HO}}(T)$ and $Q^{\text{Pert}}(T)/Q^{(0)}(T)$ for temperatures ranging from 50 to 500 K. For 1,3-butadiene, the conventional harmonic oscillator partition function differs from $Q^{\text{Pert}}(T)$ by over 20% for temperatures near 500 K.

for any J value can be approximately obtained by letting the rotational energy $E_{J,m}$ depend only on J and the m th eigenvalue of the large-amplitude torsion. Therefore, the energy of a particular rovibrational state is given by

$$E_{J,m,n} = E_{J,m} + E_{m,n}^{(0)} + E_{m,n}^{(1)} \\ = E_{J,m} + E_m + \hbar \sum_{k=1}^{3N-7} \left\{ \left[\omega_k(s_0) + \langle \psi_m(s) | \omega_k(s) - \omega_k(s_0) | \psi_m(s) \rangle \right] n_k + \frac{1}{2} \omega_k(s_0) \right\}. \quad (11)$$

In this approximation, the canonical partition function becomes

$$Q^{\text{Pert}}(T) = \sum_{J,m,n} \exp \left\{ - \left[E_{J,m,n} - \hbar \sum_{k=1}^{3N-7} \frac{1}{2} \omega_k(s_0) \right] \times k_B T \right\} \\ = \sum_{J,m,n} \exp \left(- \left\{ E_{J,m} + E_m + \hbar \sum_{k=1}^{3N-7} [\omega_k(s_0) + \langle \psi_m(s) | \omega_k(s) - \omega_k(s_0) | \psi_m(s) \rangle] n_k \right\} \times k_B T \right). \quad (12)$$

The partition functions in this paper are defined with the zero of energy at the lowest quantum state; hence, the partition function is bounded from below by unity. This is the standard choice in thermodynamic tables when calculating Gibbs free energies, entropies, and heat capacities. The summation over the set of $3N-7$ projected harmonic quantum numbers is a geometric series and can be summed exactly to give

$$Q^{\text{Pert}}(T) = \sum_m \left[\exp(-E_m/k_B T) \sum_J \exp(-E_{J,m}/k_B T) \prod_{k=1}^{3N-7} q_{\text{vib},m,k}(T) \right] \\ = \sum_m \left[\exp(-E_m/k_B T) q_{\text{rot},m}(T) \prod_{k=1}^{3N-7} q_{\text{vib},m,k}(T) \right], \quad (13)$$

where

$$q_{\text{vib},m,k}(T) = \frac{1}{1 - \exp\{-\hbar[\omega_k(s_0) + \langle \psi_m(s) | \omega_k(s) - \omega_k(s_0) | \psi_m(s) \rangle] \times k_B T\}} \quad (14)$$

is a modified partition function for the k th projected vibrational mode, and

$$q_{\text{rot},m}(T) = \frac{1}{\sigma} \left(\frac{2k_B T}{\hbar^2} \right)^{3/2} \{ \pi \langle \psi_m(s) | \det[\mathbf{I}_0(s)] | \psi_m(s) \rangle \}^{1/2} \quad (15)$$

is a modified partition function for the external rotation, which is allowed to depend only on the m th eigenstate of the large-amplitude torsion. The variable σ ($= 2$ for 1,3-butadiene) is the rotational symmetry number that prevents overcounting of indistinguishable configurations in classical phase space. Additionally, the partition function in eq. (15) approximately takes into account the coupling between internal and external rotation by replacing the equilibrium products of inertia $I_{0a}I_{0b}I_{0c}$ by the torsional-averaged quantity

$$I_{\text{eff},m} = \langle \psi_m(s) | \det[\mathbf{I}_0(s)] | \psi_m(s) \rangle. \quad (16)$$

Conventionally, the rotational constants used in the standard rotational partition function are evaluated from the inertia tensor at the equilibrium geometry. Since the rotational constants depend strongly on the internal rotation coordinate for asymmet-

Table 1. Comparison of Gibbs Free Energy Values for 1,3-Butadiene at Various Temperatures.

	50 K	100 K	150 K	200 K	273.15 K	300 K	400 K	500 K
Ref. 26/(kJ mol ⁻¹)	-7.95	-18.29	-29.70	-41.93	-61.10	-68.50	-97.75	-129.59
$G^{\text{Pert}}/(\text{kJ mol}^{-1})$	-7.94	-18.27	-29.66	-41.86	-60.98	-68.35	-97.44	-129.05
$G^{(0)}/(\text{kJ mol}^{-1})$	-7.94	-18.26	-29.66	-41.86	-60.96	-68.32	-97.37	-128.91
$G^{(\text{HO})}/(\text{kJ mol}^{-1})$	-7.94	-18.26	-29.63	-41.81	-60.87	-68.21	-97.08	-128.30

The free energy values for each of the three models (Pert, (0), and HO) were calculated using the same molecular geometries, energies, and frequencies at the CCSD(T)//MP2 level of theory.

Table 2. Comparison of Entropy Values for 1,3-Butadiene at Various Temperatures.

	50 K	100 K	150 K	200 K	273.15 K	300 K	400 K	500 K
Ref. 26/(J K ⁻¹ mol ⁻¹)	192.63	218.82	236.84	251.89	272.07	279.28	305.63	330.80
$S^{\text{Pert}}/(\text{J K}^{-1} \text{ mol}^{-1})$	192.36	218.51	236.49	251.37	271.06	278.06	303.65	328.28
$S^{(0)}/(\text{J K}^{-1} \text{ mol}^{-1})$	192.34	218.47	236.43	251.26	270.82	277.76	303.08	327.44
$S^{(\text{HO})}/(\text{J K}^{-1} \text{ mol}^{-1})$	192.28	218.25	236.11	250.80	269.93	276.61	300.66	323.59

ric rotors, this effect can be incorporated by evaluating the determinant of the inertia tensor averaged over the large-amplitude wavefunctions.²⁴

Figure 3 shows the variation of $I_{\text{eff},m}$ for the lowest 100 torsional states for 1,3-butadiene. The dotted horizontal line is the numerical value for the rigid rotor products of inertia $I_{0a}I_{0b}I_{0c}$ evaluated at the *trans* conformation. For 1,3-butadiene, the 32nd rotor level is the first torsional level above the highest barrier to rotation. For $m < 7$, $I_{\text{eff},m}$ does not vary appreciably since the torsional wavefunction is localized in the *trans* global minimum. For $7 < m < 32$, $I_{\text{eff},m}$ varies rapidly between two limits since the torsional wavefunction alternates between the two *gauche* local minima and the single *trans* minimum. The two pairs of points near $I_{\text{eff},m} \approx 2.23 \times 10^5$ (amu Å²)³ correspond to the two torsional-averaged *gauche* effective inertias and the single points near $I_{\text{eff},m} \approx 2.00 \times 10^6$ (amu Å²)³ are the averaged *trans* effective inertias. For $m > 32$, the torsion is nearly a free rotation, and $I_{\text{eff},m}$ is approximately constant with a limiting value of approximately 2.06×10^6 (amu Å²)³. Figure 3 indicates the value of $I_{\text{eff},m}$ is 25% larger than the equilibrium products of inertia $I_{0a}I_{0b}I_{0c}$ when $m > 32$; using the conventional rigid rotor inertias may incur significant errors in the external rotational partition function alone.

The matrix expressions defined in eqs. (8–15) are naturally suited for programming in a high-level matrix manipulation language such as MATLAB. However, a large set of energy eigenvalues is required so that the error due to the limited number of states included in the partition function is negligible for the higher temperatures of interest. The corresponding set of eigenvectors is also necessary in this computation in order to calculate the perturbations and expectation values defined in eqs. (9) and (16), respectively. As a result, these massive computations were performed in a highly parallelized manner with MATLAB software enabled by the new STAR-P interactive parallel computing platform provided by Interactive Supercomputing, Inc. Detailed descriptions of STAR-P and its software architecture has been given by Choy and Edelman.^{10,11} For the present work on 1,3-butadiene, a large set of eigenvalues and eigenvectors for

the Hamiltonian defined in eq. (5) were computed by diagonalizing a double-precision 20,001 × 20,001 matrix.

The novelty of this procedure lies in the use of a high-level matrix manipulation language to compose the equations and allowing the STAR-P platform to transform the high-dimensional MATLAB manipulations into parallelized codes easily executed on workstation clusters. The high-level STAR-P system allows easy implementation of eqs. (8)–(15) by providing the look of a MATLAB interface but the power of several workstation computers. For this work, all codes were written in regular MATLAB m-files and automatically converted by the STAR-P program to run on an SGI Altix 350 server which comprises 16 Itanium 2 processors (1.0 Ghz) and 80 GB of RAM. One of the many bottlenecks associated with obtaining all 20,001 eigenvalues and 20,001 × (3N–7) perturbations is the storage and subsequent diagonalization of the Hamiltonian matrix. To remove this computational difficulty, the STAR-P software automatically partitions the Hamiltonian in blocks that are computed and stored with distributed memory. Finally, an automatic administration process controls the load-balance of the computing nodes and distributes the needed data to be diagonalized and matrix-multiplied in parallel. Using the obtained energy eigenvalues and expectation values, the partition function defined in eq. (13) was easily computed.

Figure 4 shows the ratios of $Q^{\text{Pert}}(T)/Q^{\text{HO}}(T)$ and $Q^{\text{Pert}}(T)/Q^{(0)}(T)$ as a function of temperature where $Q^{\text{HO}}(T)$ is the conventional harmonic oscillator, rigid rotor partition function, $Q^{(0)}(T)$ results from summations of energies in eq. (7), and $Q^{\text{Pert}}(T)$ is the partition function defined in eq. (13). In both $Q^{\text{HO}}(T)$ and $Q^{(0)}(T)$ the equilibrium products of inertia $I_{0a}I_{0b}I_{0c}$ were used in the rotational partition function. The conventional harmonic oscillator partition function from the raw *ab initio* calculations differs from $Q^{\text{Pert}}(T)$ by over 20% for temperatures up to 500 K. The more reasonable approximation of $Q^{(0)}(T)$ deviates from $Q^{\text{Pert}}(T)$ much less than $Q^{\text{HO}}(T)$, but there is still a 4% difference. As a result, the neglect of the various torsionally-averaged quantities in eqs. (9) and (16) can incur serious errors if applied to high-temperature conditions.

Table 3. Comparison of Heat Capacity Values for 1,3-Butadiene at Various Temperatures.

	50 K	100 K	150 K	200 K	273.15 K	300 K	400 K	500 K
Ref. 26/(J K ⁻¹ mol ⁻¹)	35.09	41.31	48.28	57.14	73.70	80.27	103.44	122.09
$C_p^{\text{Pert}}/(\text{J K}^{-1} \text{ mol}^{-1})$	34.98	41.30	48.00	56.15	71.56	77.86	100.81	119.84
$C_p^{(0)}/(\text{J K}^{-1} \text{ mol}^{-1})$	34.98	41.26	47.89	55.91	70.97	77.12	99.67	118.62
$C_p^{(\text{HO})}/(\text{J K}^{-1} \text{ mol}^{-1})$	34.79	41.02	47.60	55.18	68.61	73.99	93.98	111.76

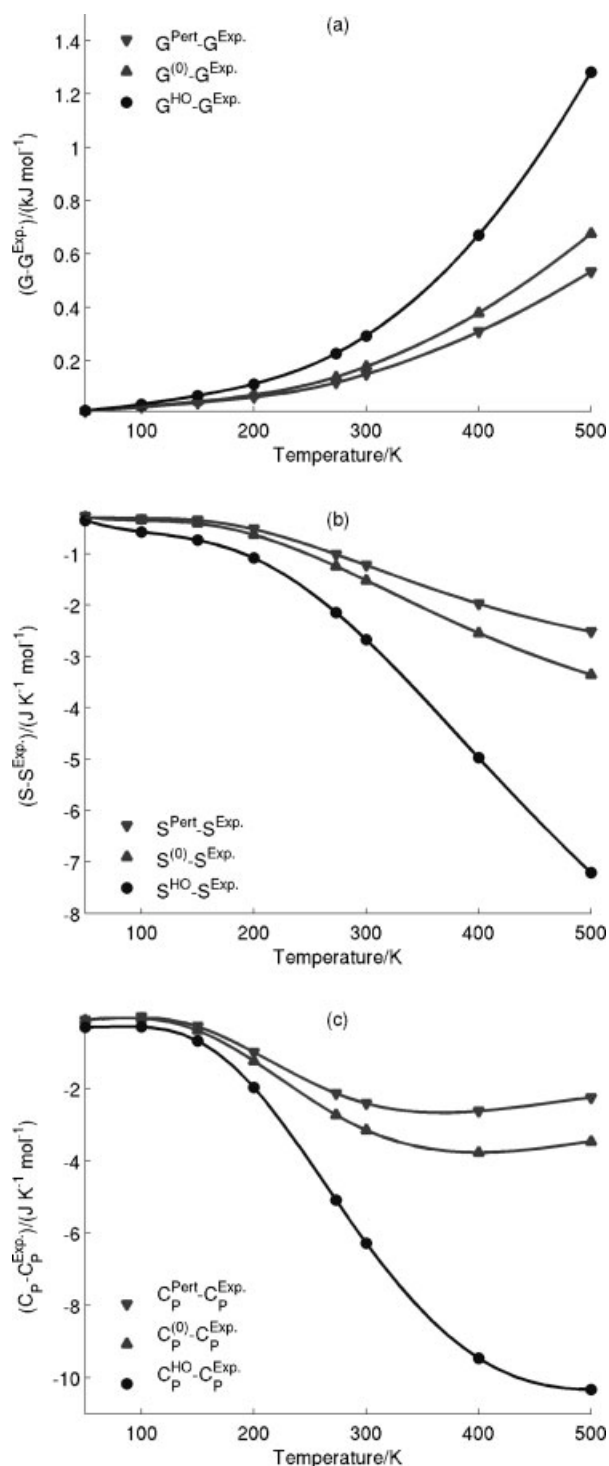


Figure 5. (a)–(c) Deviations of free energies, entropies, and heat capacities from tabulated thermodynamic values of 1,3-butadiene. Each of the three curves was obtained using the methods described in the results section; in all the cases considered, the deviations are smallest for the perturbative expressions.

As a final application of our results for a large-amplitude asymmetric torsion, the thermodynamic functions for the Gibbs free energy, entropy, and heat capacity of 1,3-butadiene can be directly calculated from the canonical partition function:

$$G(T) = -RT \ln[Q(T)], \quad (17)$$

$$S(T) = R \ln[Q(T)] + RT \frac{\partial \ln[Q(T)]}{\partial T}, \quad (18)$$

$$C_p(T) = 2RT \frac{\partial \ln[Q(T)]}{\partial T} + RT^2 \frac{\partial^2 \ln[Q(T)]}{\partial T^2} + R, \quad (19)$$

where R is the ideal gas constant, and $Q(T)$ implicitly includes a contribution due to translation, which is always separable from vibration and rotation. The numerical values of $G(T)$, $S(T)$, and $C_p(T)$ each computed from the different partition functions $Q^{(0)}(T)$, $Q^{\text{HO}}(T)$, and $Q^{\text{Pert}}(T)$ are given in Tables 1–3. The first row of each table gives the experimental values recommended by the National Institute of Standards and Technology²⁵ found in standard thermodynamic reference data.²⁶ The data compiled in the standard thermodynamic references are sometimes obtained by averaging several experimentally calculated values; as a result, the error for each data set is difficult to quantify, and the reference data should not be expected to be better than 1% from the best experimental results. The effect of the perturbative results (Pert) in the thermodynamic properties of 1,3-butadiene is also shown in Figures 5a–5c to compare with the zeroth-order (0) and harmonic approximations (HO). The deviation from the experimental values (Exp.) is similar in all three cases with the perturbative results being closest to the tabulated values followed by the zeroth-order and harmonic approximations. Among the three thermodynamic functions G , S , and C_p , we observe considerable quantitative differences between the approximate methods in calculating the Gibbs free energy. This result can be understood realizing that the error in $\ln(Q)$ is higher and increases faster than its temperature derivatives $\partial \ln(Q)/\partial T$ and $\partial^2 \ln(Q)/\partial T^2$. Therefore, the use of a harmonic oscillator approximation will incur more error in the Gibbs free energy than in heat capacity values.

Conclusions

We have presented a simple approach to construct partition functions and thermochemical properties for the situation where a large-amplitude motion is coupled to both a set of small-amplitude vibrations and the external rotation of a molecule. This theoretical treatment is based on the internal coordinate path kinetic energy operator with the corresponding potential energy obtained from an *ab initio* computational method. Using this formulation of the coordinate path, we have applied a perturbative approach to study 1,3-butadiene since it provides an excellent model for a highly coupled system with a very large configuration space (23 vibrational modes coupled to a torsion).

One of the more important aspects of our implementation is the use of the new STAR-P interactive parallel computing platform to easily transform our simple MATLAB scripts into parallelized codes easily executed on workstation clusters. Having these programs written in a familiar high-level language permits easy modification of the MATLAB scripts for applications with even larger systems. Of course, the predictions of a theoretical model should be consistent with the experimental observations to which the model is applied. A comparison of computed Gibbs free energies, entropies, and heat capacities for 1,3-butadiene against experimental data indicates the perturbative expressions are more accurate than the zeroth-order or harmonic oscillator approximations for all the cases considered. In conclusion, the practical feature that makes this method feasible for even very large molecules is that it requires a relatively modest number of calculations—algorithms for evaluating second derivatives in quantum chemistry calculations are now efficient and routine, and the use of high-level programs makes this approach useful for polyatomic systems.

The MATLAB scripts used to run the STAR-P interactive parallel computing platform can be obtained upon request from the corresponding author.

Acknowledgments

All *ab initio* calculations were performed on a custom-built server at the Sidney-Pacific Residence at the Massachusetts Institute of Technology, which comprises 2 processors (2×2.8 GHz Intel Xeon), with a total of 4 Gb of RAM. All other calculations and algorithm developments were performed on a parallelized version of MATLAB using STAR-P from Interactive Supercomputing, Inc. The authors are grateful to Joan Puig Giner and Dr. Vern Shrauger for helping parallelizing our MATLAB codes to run on the M.I.T. ACES SGI Altix 350 server.

References

1. Hnizdo, V.; Fedorowicz, A.; Singh, H.; Demchuk, E. *J Comput Chem* 2003, 24, 1172.
2. Darian, E.; Hnizdo, V.; Fedorowicz, A.; Singh, H.; Demchuk, E. *J Comput Chem* 2005, 26, 651.
3. Tafipolsky, M.; Schmid, R. *J Comput Chem* 2005, 26, 1579.
4. Liu, M. H.; Chen, C. *J Comput Chem* 2006, 27, 537.
5. Pitzer, K. S.; Gwinn, W. D. *J Chem Phys* 1942, 10, 428.
6. Pitzer, K. S. *J Chem Phys* 1946, 14, 239.
7. Pitzer, K. S.; Kilpatrick, J. E. *J Chem Phys* 1949, 17, 1064.
8. Tew, D. P.; Handy, N. C.; Carter, S.; Irlé, S.; Bowman, J. M. *Mol Phys* 2003, 101, 3513.
9. Kraka, E.; Wu, A.; Cremer, D. *J Phys Chem A* 2003, 107, 9008.
10. Choy, R.; Edelman, A. *Proc IEEE* 2005, 93, 331.
11. <http://www.interactivesupercomputing.com>. Last accessed on 4 July 2006.
12. Miller, W. H.; Handy, N. C.; Adams, J. E. *J Chem Phys* 1980, 72, 99.
13. Wong, B. M.; Thom, R. L.; Field, R. W. *J Phys Chem A* 2006, 110, 7406.
14. Frisch, M. J.; Trucks, G. W.; Schlegel, H. B.; Scuseria, G. E.; Robb, M. A.; Cheeseman, J. R.; Montgomery, J. A., Jr.; Vreven, T.; Kudin, K. N.; Burant, J. C.; Millam, J. M.; Iyengar, S. S.; Tomasi, J.; Barone, V.; Mennucci, B.; Cossi, M.; Scalmani, G.; Rega, N.; Petersson, G. A.; Nakatsuji, H.; Hada, M.; Ehara, M.; Toyota, K.; Fukuda, R.; Hasegawa, J.; Ishida, M.; Nakajima, T.; Honda, Y.; Kitao, O.; Nakai, H.; Klene, M.; Li, X.; Knox, J. E.; Hratchian, H. P.; Cross, J. B.; Bakken, V.; Adamo, C.; Jaramillo, J.; Gomperts, R.; Stratmann, R. E.; Yazyev, O.; Austin, A. J.; Cammi, R.; Pomelli, C.; Ochterski, J. W.; Ayala, P. Y.; Morokuma, K.; Voth, G. A.; Salvador, P.; Dannenberg, J. J.; Zakrzewski, V. G.; Dapprich, S.; Daniels, A. D.; Strain, M. C.; Farkas, O.; Malick, D. K.; Rabuck, A. D.; Raghavachari, K.; Foresman, J. B.; Ortiz, J. V.; Cui, Q.; Baboul, A. G.; Clifford, S.; Cioslowski, J.; Stefanov, B. B.; Liu, G.; Liashenko, A.; Piskorz, P.; Komaromi, I.; Martin, R. L.; Fox, D. J.; Keith, T.; Al-Laham, M. A.; Peng, C. Y.; Nanayakkara, A.; Challacombe, M.; Gill, P. M. W.; Johnson, B.; Chen, W.; Wong, M. W.; Gonzalez, C.; Pople, J. A. *Gaussian 03, Revision D. 01*; Gaussian: Wallingford, CT, 2004.
15. Murcko, M. A.; Castejon, H.; Wiberg, K. *J Phys Chem* 1996, 100, 16162.
16. Karpfen, A.; Choi, C. H.; Kertesz, M. *J Phys Chem A* 1997, 101, 7426.
17. Sancho-García, J. C.; Pérez-Jiménez, A. J.; Moscardó, F. *J Phys Chem A* 2001, 105, 11541.
18. Karpfen, A.; Parasuk, V. *Mol Phys* 2004, 102, 819.
19. Engeln, R.; Consalvo, D.; Reuss, J. *Chem Phys* 1992, 160, 427.
20. Saltiel, J.; Sears, D. F., Jr.; Turek, A. M. *J Phys Chem A* 2001, 105, 7569.
21. Kendall, R. A.; Dunning, T. H., Jr.; Harrison, R. J. *J Chem Phys* 1992, 96, 6796.
22. Sancho-García, J. C.; Cornil, J. *J Chem Phys* 2004, 121, 3096.
23. Konkoki, Z.; Cremer, D.; Kraka, E. *J Comput Chem* 1997, 18, 1282.
24. Papoušek, D.; Aliev, M. R. *Molecular Vibrational-Rotational Spectra*; Elsevier: New York, 1982.
25. <http://webbook.nist.gov/cgi/cbook.cgi?ID=C106990&Units=SI&Mask=1#Thermo-Gas>. Last accessed on 4 July 2006.
26. Thermodynamics Research Center. Selected Values of Properties of Chemical Compounds; Thermodynamics Research Center: College Station, TX, 1997.